Electronic Supplementary Material (ESI) for Physical Chemistry Chemical Physics.

Exploring the nature of the liquid-liquid transition in silicon: A non-activated transformation

(Supplementary Information)

Yongjun Lü[1,4*], Xiangxiong Zhang[2], Min Chen[2] and Jianzhong Jiang[3,4]

[1]*School of Physics, Beijing Institute of Technology, Beijing 100081, P. R. China*
[2]*Department of Engineering Mechanics, Tsinghua University, Beijing 100084, P. R. China*
[3]*International Center for New-Structured Materials (ICNSM), Zhejiang University and Laboratory of New-Structured Materials, Department of Materials Science and Engineering, Zhejiang University, Hangzhou 310027, P. R. China*
[4]*State Key Laboratory of Silicon Materials, Zhejiang University, Hangzhou, 310027, P. R. China*

*To whom correspondence should be addressed
E-mail: 04537@bit.edu.cn

1. Identification of large-volume atoms

We identify the LDL silicon in terms of the characteristic of low density. A direct path is identifying the large-volume atoms using the Voronoi polyhedron method. However, the Voronoi volume, V_i (i denotes atom i), cannot effectively distinguish the large-volume atoms belonging to LDL from the HDL environment. Figures 1a and b show the probability distributions of the Voronoi volume for the normal liquid and the crystalline Si-I as well as for the normal liquid and the LDL phase. The overlaps between them are serious, thus, it is difficult to distinguish the low-density region using the Voronoi polyhedron method.

The average atomic volume defined in equation (1) involves the volume information of the neighboring atoms, and is expected to diminish the effect of the volume fluctuation. Figures S1c and d show the results for the cases presented in Figs. S1a and b. It can be seen that the overlaps are considerably reduced. We define the atoms with V_i>19.6 Å^3 as large-volume atoms, which ensure that most atoms in the low-density region are identified.

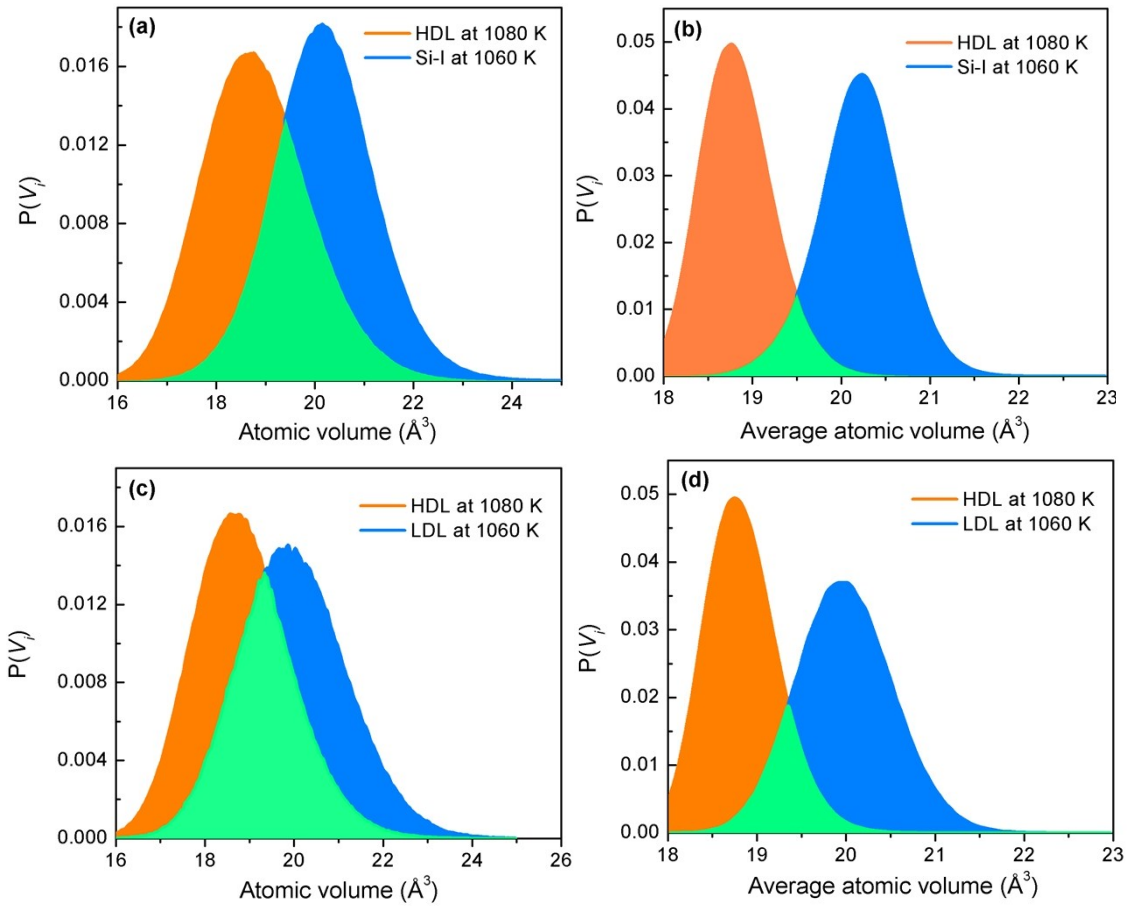

Fig. S1. Identification of large-volume atoms. (a) The probability distributions of Voronoi atomic volume above and below crystallisation. (b) The probability distributions of average atomic volume using the definition of equation (1). (c) and (d) show the probability distributions of HDL and LDL silicon above and below the HDL-LDL transformation. The overlaps are significantly reduced using the average atomic volume, thus, the average method can effectively improve the accuracy of identifying low-density clusters.

2. Identification of LDL silicon

To confirm that the LDL silicon obtained in our simulations is identical to that reported in the previous studies, we check the thermodynamic, structural and dynamic appearance.

2.1 Density change

The low-density silicon is obtained via quenching liquid silicon from 2000 K to 1300 K at a cooling rate of 100 K per 1.2 ns, and then continues to 900 K at a rate of 20 K per 1.2 ns. The configuration is recorded every 2000 MD steps and a total of 600 configurations are sampled at each temperature. The density is produced by averaging the 600 configurations. The quenching is carried out in the negative pressure range from 0 to -1.6 GPa. Figure S1a shows the density as a function of temperature at the five example pressures. The transitions from HDL to LDL are observed. The density of LDL silicon shows a decrease with increasing tensile stress. The systems are quenched at four different cooling rates: 10 K per 0.1, 0.8, 1.2 and 2.0 ns from 1300 K. The density of LDL silicon depends on cooling rate: a higher cooling rates lead to a larger density of LDL. When the cooling rate is decreased to 10 K per 2.0 ns, the crystallization of Si-I occurs instead of the HDL-LDL transition (P=0 GPa), as shown in Fig. S2b. The

density changes across the transition are identical with the published results [Beaucage, P. & Mousseau, N. *J. Phys.: Condens. Matter* **17**, 2269 (2005)].

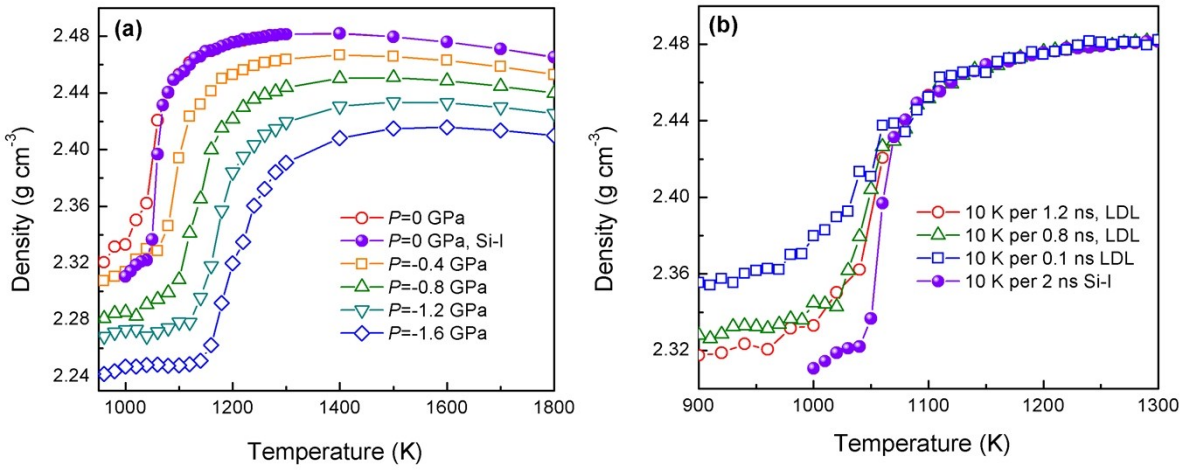

Fig. S2. Density of liquid silicon as a function of temperature. (a) Effect of pressure on density at the cooling rate of 10K per 1.2 ns. For comparison, the density change during crystallization at zero pressure is presented as solid circles. (b) Effect of cooling rate on density at zero pressure.

2.2 Radial distribution function and structure factor

A common description of the global structure is provided by the radial distribution functions (RDF), which measures the averaged particle density as a function of distance from a central atom and is given by

$$g(r) = \frac{n(r)}{4\pi r^2 \rho \Delta r} \tag{S1}$$

where $n(r)$ is the atom number between r and $r+\Delta r$, ρ is the number density of the system. Figure S3a shows the RDFs of HDL, LDL and crystalline Si-I. The RDF of LDL is consistent with the reported results [Sastry, S & Angell, C. A. *Nature Mater.* **2**, 739 (2003); Ganesh, P. & Widom, M. *Phys. Rev. Lett.* **102**, 075701 (2009); Jakse, N. & Pasturel, A. *Phys. Rev. Lett.* **99**, 205702 (2007)] . Using the RDF, the structure factor is given by

$$S(q) = 1 + \frac{4\pi\rho}{q}\int_0^\infty [g(r)-1]\sin(qr)\mathrm{d}r \ , \tag{S2}$$

where q is the wave vector. Figure S3b shows $S(q)$ of HDL, LDL and the system in the transition to LDL. For the sake of comparison, $S(q)$ of Si-I is calculated. The characteristic features of the $S(q)$ curves are identical to the results provided by the first-principle simulations [Ganesh, P. & Widom, M. *Phys. Rev. Lett.* **102**, 075701 (2009)].

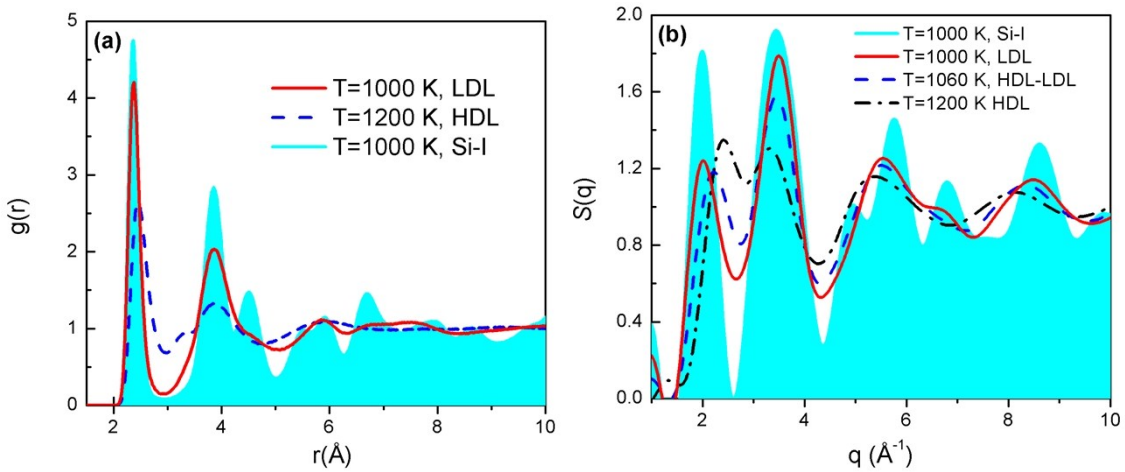

Fig. S3. Radial distribution function and structure factor. (a) Radial distribution functions, $g(r)$ for LDL, HDL and Si-I. (b) Structure factors, $S(q)$ for HDL, LDL, SI-I as well as the system in the transition from HDL to LDL phase at 1060 K. Both radial distribution functions and structure factors are identical with the reported results [Ganesh, P. & Widom, M. *Phys. Rev. Lett.* 102, 075701 (2009)].

2.3 Coordination number

The coordination number is calculated by counting the atom number within the nearest-neighboring distance, r_c that is determined by the RDF. Figure S4 shows the coordination number as a function of temperature at zero pressure for both LDL and Si-I. The coordination number of LDL and Si-I is 4.2 and 4.0, respectively, which is in good agreement with the previous simulations [Vasisht, V. V., Saw, S. & Sastry, S. *Nature Phys.* **7**, 549 (2011)].

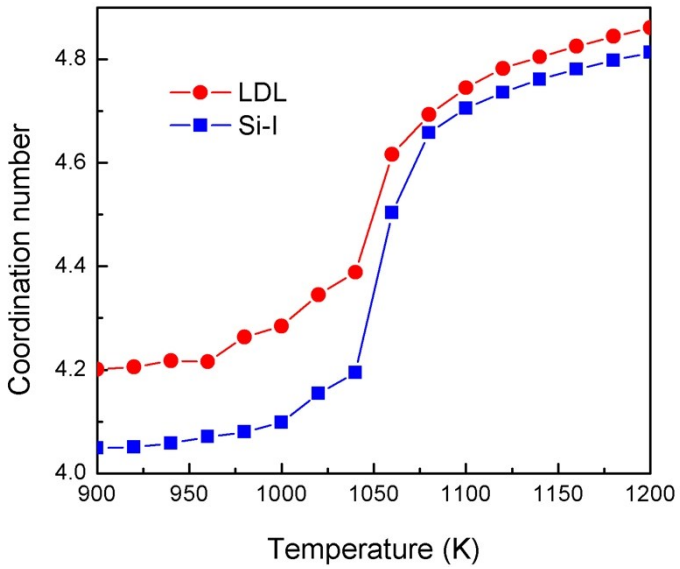

Fig. S4. Coordination number versus temperature. The coordination number changes in the HDL-LDL transition and the crystallization are presented. The coordination number is obtained from the ensemble average on atom number within the nearest-neighboring shell.

2.4 Diffusion coefficients

The diffusion coefficients of silicon are calculated by the long-time limit of the mean-squared displacement (MSD),

$$D = \frac{1}{6N}\lim_{t\to\infty}\sum_{i=1}^{N}\frac{1}{t}\left\langle \left| r_i(t) - r_i(0) \right|^2 \right\rangle \tag{S3}$$

where $r_i(t)$ and $r_i(0)$ are the positions of atom i at time t and 0 respectively, N is the atom number. In the simulations, the atomic configuration is recorded every 2 ps (2000 MD steps), and MSD is averaged for 100 measurements with the time interval of 200 ps. Then the self-diffusion coefficient is achieved from the convergence of Eq. S3 to asymptotic behavior. Figure S5 shows the diffusion coefficients as a function of the inverse of temperature. Across the transition, the diffusion coefficients of LDL silicon are in the order of magnitude of 10^{-8} cm^2s^{-1}, featuring a viscous liquid, which is comparable to the other results in the order of magnitude. The diffusion tends to be slowed down with increasing tensile stress, as shown in Fig. S5. The pressure dependence of diffusion coefficients shows that the transition occurs at higher temperature as the tensile stress increases.

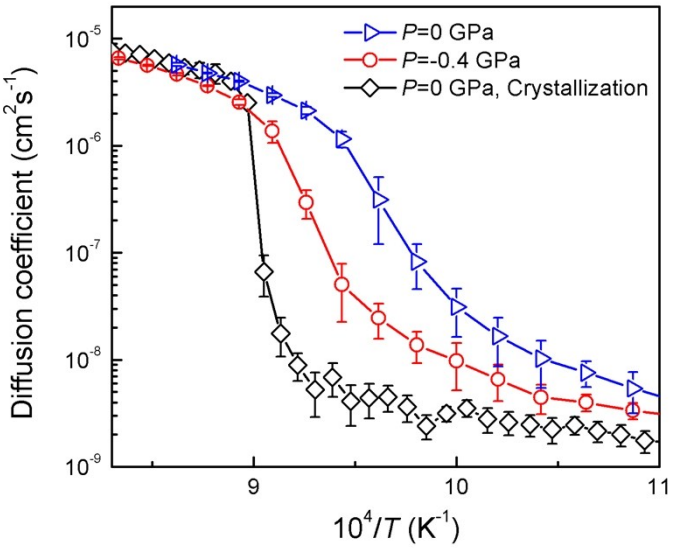

Fig. S5. Diffusion coefficient. The diffusion coefficients are plotted as a function of the inverse of temperature at P = 0 and -0.4 GPa. The diffusion coefficients of LDL phase are in the order of 10^{-8} cm^2 s^{-1}, and one order of magnitude larger than the values of crystalline Si-I. The negative pressure tends to decrease the diffusion coefficient, leading to the occurrence of HDL-LDL transition at higher temperature.

2.5 Intermediate scattering function

The intermediate scattering function is defined by

$$F(q,t) = \frac{1}{N}\left\langle \rho(q,t)\rho(-q,0) \right\rangle \tag{S4}$$

where $\rho(q,t) = \sum_j \exp\left(-iq\cdot r_j(t)\right)$. The intermediate scattering function is related to the structure factor by

$F(q,0) = S(q)$. Figure S6 shows the intermediate scattering function of HDL and LDL. The curve of LDL displays a distinct β-relaxation process, suggesting a fragile-to-strong transition of supercooled silicon accompanying the LDL transition.

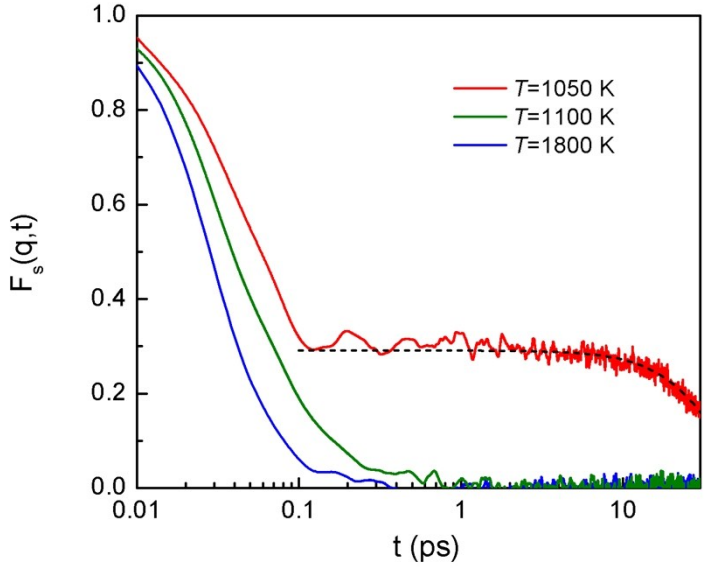

Fig. S6. Intermediate scattering function. The intermediate scattering function, $F_s(q,t)$ is simulated at T=1800, 1100 and 1050 K, respectively and q is the wave-vectors. The curve for the LDL phase (red) shows the β-relaxation. The dashed line is a fitting to the Kohlrausch-Williams-Watts (KKW) relaxation function, $F_s(q,t) = A\exp\left[-(t/\tau)^{\beta}\right]$, β and τ are the stretched exponent and the structural relaxation time, respectively.

3. Calculating the fractal dimension

The box fractal dimension of the LDL network is calculated by the following method. Define a parameter, δ_i as

$$\delta_i = \frac{\left\| X_{\max} - X_{\min} \right\|}{i} \qquad (i = 1, 2 \mathrm{L}\ n) \tag{S5}$$

where $X_{\max}$=max(r_x, r_y, r_z) and $X_{\min}$=min(r_x, r_y, r_z). Then, we place a set of box with the side length of δ_i to the simulation cell with the common origin and count the atom number in the ith box, $N(\delta_i)$. The box fractal dimension, D_f is given by

$$D_f = \sum_{i=0}^{n-1} \left[\log N_i(\delta_i) \cdot \log \delta_i \right] \Big/ \sum_{i=0}^{n-1} \log \delta_i^2 \tag{S6}$$

Figure S7 shows the box fractal dimension as a function of temperature.

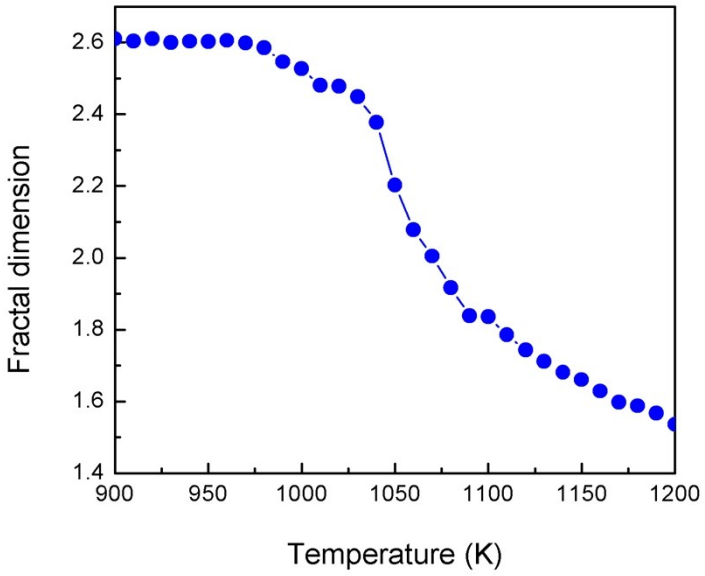

Fig. S7. Fractal dimension of LDL framework. The box fractal dimension continuously increases to 2.6 through the HDL-LDL transition, indicating the LDL framework has a three-dimensional configuration.

4. Nucleation rate and nucleation barrier

For the sake of comparison, we evaluate the MFPT of the nucleation process, by which we calculate the nucleation rate and the free energy barrier (nucleation barrier). Table S1 list the parameters associated with nucleation of Si.

Table S1. The size of critical nuclei n^*, the fitting parameter c in Eq. 5, the system volume V, the nucleation rate per unit time and volume J_V, and the nucleation barrier ΔG for N=1000, 2744 and 4096.

N	n^*	c	V ($\times 10^4$ Å^3)	J_V ($\times 10^{33}$ s^{-1}m^{-3})	ΔG (k_BT)
1000	63	0.01149	2.021	7.061	3.89
2744	65	0.01155	5.549	4.193	2.14
4096	61	0.01527	7.702	2.885	1.70